Earthq Eng & Eng Vib (2021) 20: 291-302 **DOI**: https://doi.org/10.1007/s11803-021-2020-0

Functionality analysis of an urban water supply network after strong earthquakes

Li Jichao[1†], Shang Qingxue[1‡], Hou Guanjie[2‡], Li Quanwang[2§] and Wang Tao[1*]

1. *Key Laboratory of Earthquake Engineering and Engineering Vibration, Institute of Engineering Mechanics, China Earthquake Administration, Harbin 150080, China*
2. *Department of Civil Engineering, Tsinghua University, Beijing 100084, China*

Abstract: An urban water supply network (WSN) is a crucial lifeline system that helps to maintain the normal functioning of modern society. However, the hydraulic analysis of a significantly damaged WSN that suffers from pipe breaks or leaks remains challenging. In this paper, a probability-based framework is proposed to assess the functionality of WSNs in the aftermath of powerful earthquakes. The serviceability of the WSN is quantified by using a comprehensive index that considers nodal water flow and nodal pressure. This index includes a coefficient that reflects the relative importance of these two parameters. The demand reduction (DR) method, which reduces the water flow of nodes while preventing the negative pressure of nodes, is proposed. The difference between the negative pressure elimination (NPE) method and the DR method is discussed by using the example of a WSN in a medium-sized city in China. The functionality values of the WSN are 0.76 and 0.99 when nodal pressure and nodal demands are used respectively as the index of system serviceability at an intensity level that would pertain to an earthquake considered to occur at a maximum level. When the intensity of ground motion is as high as 0.4 g, the DR method requires fewer samples than the NPE method to obtain accurate results. The NPE method eliminates most of the pipes, which may be unrealistic.

Keywords: water supply network; system serviceability; hydraulic analysis; negative pressure elimination; benchmark city

1 Introduction

Urban water supply networks (WSNs), in conjunction with other lifeline systems, such as power, transportation, and communication systems, are indispensable for maintaining the normal functioning of modern society. However, extensive damage to WSN components, especially buried pipelines, has been observed in several earthquakes, such as the 1976 Tangshan earthquake (Liu, 1986), the 1994 Northridge earthquake (EERI, 1995), the 1995 Kobe earthquake (Shinozuka, 1995), and the 2008 Wenchuan earthquake (Guo *et al*., 2008; Li *et al*., 2008). The damage substantially affected the lives and activities of residents, hindered earthquake relief work, and even caused secondary disasters (Scawthorn, 2011). Therefore, it is necessary to investigate the seismic performance of WSNs.

The seismic reliability of WSNs has been investigated in two major aspects: connectivity analysis, based on the network topological relationship (Li, 2005), and hydraulic analysis, focusing on the water delivery (Wang *et al*., 2009). Hydraulic models estimate the serviceability of the WSN by determining changes in water pressure at the supply nodes, thus leading to more realistic operational conditions of the WSN (Xu and Goulter, 1998; Chen and Li, 2004).

The hydraulic analysis of WSNs under normal operations is relatively mature when applying with the demand-driven (DD) method, which assumes that the demands are always satisfied even if pressure is insufficient. Open-source software such as EPANET (Rossman, 2000) is available to the public. However, this particular software is designed for undamaged systems and may predict unrealistically high negative pressures when used for damaged systems. Hwang *et al*. (1998) eliminated nodes with negative pressure in their analysis, which overestimated the nodal pressure and the water flow of the pipes because the size of the WSN was

Correspondence to: Wang Tao, Key Laboratory of Earthquake Engineering and Engineering Vibration, Institute of Engineering Mechanics, China Earthquake Administration, Harbin 150080, China
Tel: +86-316-3395256
E-mail: wangtao@iem.ac.cn
[†]Assistant Researcher; [‡]PhD candidate; [§]Professor; [*]Researcher

Supported by: Scientific Research Fund of the Institute of Engineering Mechanics (IEM), China Earthquake Administration (CEA) under Grant No. 2019EEEVL0505; the National Natural Science Foundation of China under Grant No. 51908519; and the Scientific Research Fund of the IEM, CEA under Grant No. 2019B02

Received November 24, 2020; **Accepted** February 8, 2021

reduced. Gao (2000) and Zhang (2006) used a simplified method to handle nodes with negative pressure. The no-flow nodes were eliminated, whereas the pressure of the partial-flow nodes was set to zero. Markov *et al*. (1994), Shi and O′Rourke (2008), and Javanbar (2008) used an iterative procedure to prevent negative pressure. The no-flow node with the highest negative pressure was eliminated one node at a time until the pressure of all the nodes was positive. Although the negative pressure elimination (NPE) method is accurate, its iterations are time-consuming.

An alternative to the demand-driven (DD) method, the pressure-driven demand (PDD) model, was proposed by Zhou *et al*. (2011), in which the nodal demands are calculated based on the nodal pressure. It requires an adaptive and highly-efficient algorithm (Hou, 2014) to solve the nonlinear hydraulic equations (Chen and Li, 2003). The Quasi-PDD method, which switches nodes iteratively between constant nodes, zero-demand nodes, and (sometimes) emitters (depending on the pressure falls), was also proposed (Pathirana, 2011; Trifunovic, 2012). Both PDD and Quasi-PDD methods require the head-outflow relationship (HOR), which is recognized as system specific without a universally accepted relationship (Liu and He, 2010; Shirzad *et al*., 2013; Liu *et al*., 2015). In addition, when considering disaster scenarios, the difference between DD and PDD simulations can be drastic (Laucelli *et al*., 2012).

The demand satisfaction ratio (DSR) and the pressure satisfaction ratio (PSR), i.e., the ratios of available demand and pressure on nodes in a damaged WSN to the required levels of demand and pressure in the undamaged system, respectively, are two major indices to evaluate the serviceability of WSNs. In the literature, the DSR is preferable to the PSR, no matter whether the DD (Li *et al*., 2006; Romero *et al*., 2010; Wang and Au, 2009), the PDD (Laucelli and Giustolis, 2015), or the quasi-PDD (Yoo *et al*., 2016a) method is used. For PDD and quasi-PDD-based analysis, the use of DSR is suitable because it considers the impact of pressure. However, the reliability of WSN may be overestimated by DSR when using DD-based analysis because the influence of pressure is ignored. Javanbarg and Takada (2009) and Nuti *et al*. (2010) used the DSR and the PSR to evaluate the performance of WSNs; the results for the two indices were presented separately. Considering the significance of nodal demand and pressure, a comprehensive index is needed to quantify the system performance of WSNs.

In this study the demand reduction (DR) method, which reduces nodal demand and prevents negative pressure in a severely damaged pipeline system, is proposed. The functionality of a typical water supply system in a medium-sized city in China is assessed by using a novel comprehensive index that simultaneously considers nodal water flow and nodal pressure. Based on the case WSN, the superiority of the index and the difference in system functionality in using the NPE method and the DR method is discussed.

2 Framework of the method

2.1 Overview

The proposed method includes three steps (Fig. 1): (1) the description of the system, consisting of the network topology with the necessary components, including nodes, pipes, reservoirs, tanks, pumps, and valves; (2) a hydraulic analysis with a focus on earthquake-induced damage, i.e., pipe breaks and leaks; and (3) assessment of system functionality, including the consideration of nodal demands and pressure.

The GIS model of the WSN was transformed into an input file of EPANET, which was used to perform hydraulic analysis in pressurized pipe networks. Two methods, NPE and DR, were used to analyse post-earthquake WSN, with pipe leaks and breaks. The functionality of the WSN was assessed using a Monte Carlo simulation. The system model of the WSN was modified during the analysis by employing a MATLAB program. In this method, pipe damage was determined based on the repair rates (RR).

2.2 Introduction of EPANET

EPANET is a software application developed by the Water Supply and Water Resources Division (formerly the Drinking Water Research Division) of the U.S. Environmental Protection Agency′s National Risk Management Research Laboratory. The software can be used to perform an extended period simulation of hydraulic and water-quality behavior in pressurized pipe networks. The primary input parameters of EPANET for a WSN include the coordinates, elevations, and demands of the nodes; the coordinates, start nodes, end nodes, lengths, diameters, roughness values, and minor loss coefficients of the pipes; and the coordinates and hydraulic heads of the reservoirs. The simulation results include water flow in the pipes and the pressures at the nodes. Additional details can be found in the user manual (Rossman, 2000).

2.3 Pipe damage modelling

The seismic damage of urban water supply pipelines includes pipe breaks and leakages. A pipe cannot

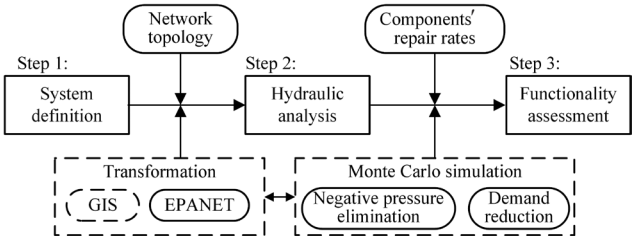

Fig. 1 Framework of the functionality assessment method of the WSN

transport water after a breakage, and the water in a broken pipe flows into the surrounding soil. By contrast, a leaking pipe can still transport water, but both water supply and water pressure are reduced. Shi and O′Rouke (2008) developed a computer program (GIRAFFE) to create hydraulic network simulations of heavily damaged water supply systems. In the GIRAFFE program, pipe leakages are classified into five categories: annual disengagement, round crack, longitudinal crack, local loss of pipe wall and local tear of pipe wall.

The pipe damage of the WSN is modelled by adding virtual joints, virtual pipes, empty reservoirs, and check valves, as shown in Figs. 2 and 3, respectively. For example, A and B are the original nodes of a pipe with a length of L. The damage occurs at the location of λL. For pipes with break damage, two new pipes, AR1 and BR2, are added to replace the broken pipe AB. The new pipes have the same parameters as the original one. However, check valves that only allow water flow from A to R1 and B to R2 are added. R1 and R2 are empty reservoirs added at the break location. Their elevation is obtained through the interpolation of the elevations of nodes A and B. For the convenience of display, the pipe AR1 is rotated counter-clockwise by 5°, which does not affect the calculation result.

For pipes with leakages, a new node, J1, and three new pipes, AJ1, BJ1, and J1R1, are added to replace the broken pipe AB. The pipes AJ1 and BJ1 have the same parameters as the original one. The length, roughness, and minor loss coefficient of pipe J1R1 are 15 cm, 1000000, and 1.0, respectively. Therefore, all energy loss from pipe J1R1 is accounted for as a minor loss (GIRAFFE user′s manual, 2008). A check valve is added so that water can only flow from the leaking pipe to the empty reservoir. The elevation of the empty reservoir R1 is the same as that of node J1 and is obtained by the interpolation of the elevations of nodes A and B.

2.4 Pipe damage generation

Due to the complexity of the WSN configuration and local site conditions, it is challenging to determine the number and locations of damage to a pipeline in an earthquake. The failure of a pipeline typically occurs due to stress concentration, which is caused by large ground deformations as a result of geotechnical failures such

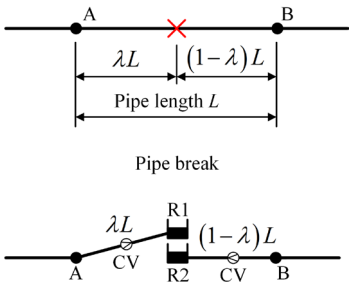

Fig. 2 Simulation method for break damage

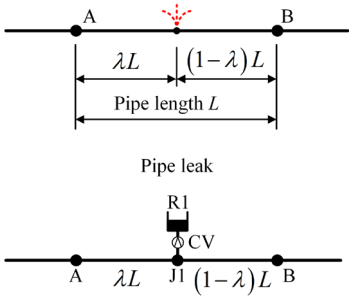

Fig. 3 Simulation method for leak damage

Table 1 Details of the virtual system

Pipe diameter (mm)	Pipe material	Number	Total length (m)
200	Cast iron	7	6,340
	PVC	0	0
300	Cast iron	60	39,285
	PVC	25	22,506
400	Cast iron	33	26,337
	PVC	57	51,265
500	Cast iron	8	6,476
	PVC	14	11,783
600	Cast iron	62	45,814
	PVC	23	22,015
800	Cast iron	11	8,545
	PVC	0	0
1000	Cast iron	22	13,703
	PVC	1	605
Sum	–	323	254,674

as landslides and liquefactions (Wham and O'Rourke, 2016). Pre-existing deterioration may further dominate failure location. Stochastic simulations of damage states of pipelines are used in the literature (Klise *et al*., 2017; Mazumder *et al*., 2020). Nevertheless, the focus of this study is not on the method for determining the damage positions. Therefore, a simpler method, as suggested by GIRAFFE, is used for a better understanding of the methodology to quantify the functionality of WSNs.

The Monte Carlo simulation technique is used to generate the damage scenarios of the WSN in three steps: (1) determine the number and locations of pipe damage, which follows a Poisson distribution; (2) assess breaks or leakages at the damage locations; (3) determine the leakage types. The types of pipe damage are determined by comparing random numbers, which are uniformly distributed between 0 and 1, and the cumulative probability of different types of damage.

The locations of pipe damage are assumed to follow a Poisson distribution (Hwang *et al*., 1998). The mean arrival rate of pipe damage is determined by the repair rate (*RR*, which is the ratio of the number of repairs and the length (km) of a pipe exposed to a seismic hazard). Assuming that pipe failure occurs randomly in the pipe segment, the distance between two adjacent leakage points, i.e., the damage interval, on pipe AB can be determined by Eq. (1) (Sheldon, 2000). The damage interval is generated one by one using random numbers. When the sum of the damage interval is greater than pipe length *L*, the locations and number of pipe damage can be determined. For example, as shown in Fig. 4, if the sum of the four damage intervals is larger than the pipe's length, three damage locations are determined. The fourth damage location will not occur because it is located outside the pipe

$$\Delta L_k = -\frac{L}{RR}\ln(1-\mathrm{rand}_k) \tag{1}$$

where ΔL_k is the k th damage interval, L is the total length of the pipe, RR is the repair rate of the pipe, and rand_k is the k th random number that is uniformly distributed between 0 (inclusive) and 1 (exclusive).

Once the locations of the pipe damage are determined, new random numbers are used to determine whether the damage is a break or a leakage. The probability of a pipe break is assumed to be 20%. If pipe leakage occurs, the type of leakage is further determined by random numbers, as listed in Table 3, which provides the probability of different types of leak damage. For example, the leakage types of a cast iron (CI) pipe are annual disengagement, round crack, longitudinal crack, and local loss of the wall if the corresponding random numbers are less than 0.3, between 0.3 and 0.8, between 0.8 and 0.9, and larger than 0.9, respectively. Note that these parameters are suggested by the GIRAFFE software, and further investigation is necessary.

Table 2 Parameters of the leak damage simulation

Damage	Virtual diameter	Recommended parameter
Annual disengagement	$2\sqrt{0.3tD}$	t=10 mm
Round crack	$\sqrt{2\theta_1}D$	θ_1=0.5°
Longitudinal crack	$2\sqrt{L_1D\theta_2/\pi}$	θ_2=0.1°, L_1=12 m
Local loss	$0.1D$	–

2.5 Negative pressure management

The EPANET hydraulic analysis algorithm is based on the laws of mass and energy conservation. The algorithm considers only the difference in the total hydraulic head, i.e., the sum of the elevation and pressure heads, to control water flow and satisfy nodal demands. As a result, unrealistically high negative pressure values may occur at some nodes, especially in an earthquake-damaged system, because the demand due to water losses from pipe breaks and leaks may be much higher than the supply from the reservoirs. Therefore, the negative pressure of the nodes must be managed. The flowchart of the NPE method, as it is implemented in GIRAFFE, and the proposed DR method are shown in Fig. 5.

2.5.1 Negative pressure elimination

In GIRAFFE, the nodes with negative pressure are eliminated in an iterative process. Nodes with negative pressures are identified after each hydraulic analysis of the damaged WSN. The node with the highest negative pressure is eliminated, as well as all connected links and control parameters associated with the node and links. In addition, the isolated nodes and links are also removed from the system if the operation causes connectivity problems. The elimination process continues until no negative pressure nodes exist in the system.

The GIRAFFE approach converts the damaged

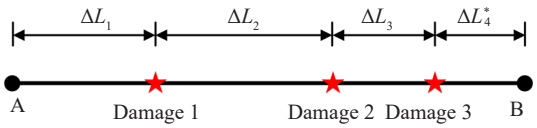

Fig. 4 Determining the pipe damage locations

Table 3 Probability of different types of leak damage

Damage	Cast iron	PVC
Annual disengagement	0.3	0.8
Round crack	0.5	–
Longitudinal crack	0.1	0.1
Local loss	0.1	0.1

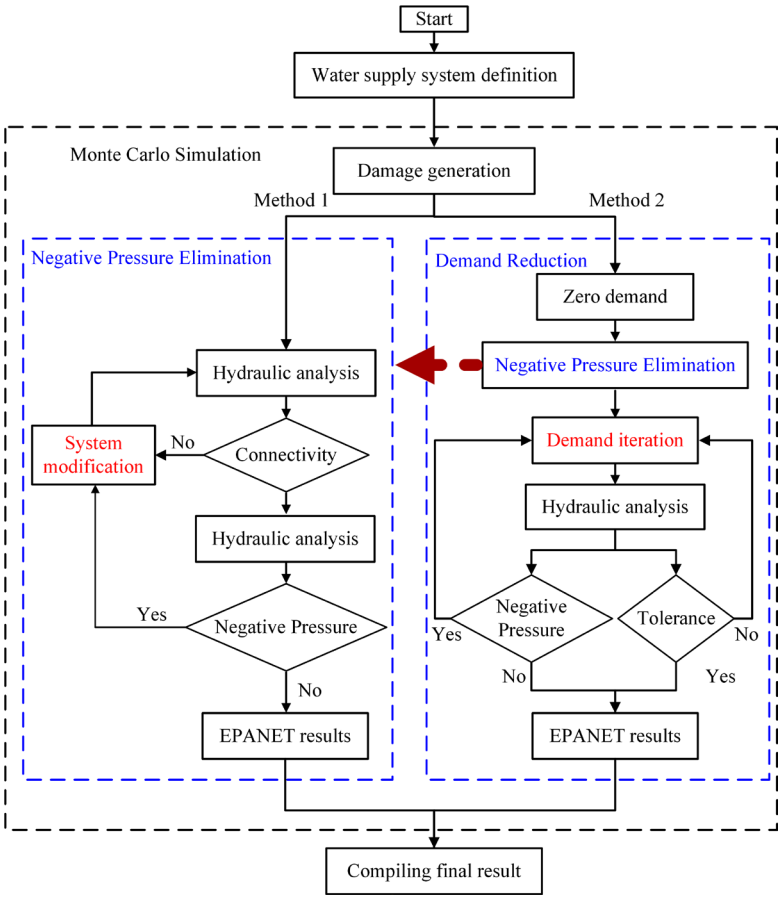

Fig. 5 Flowchart of the proposed method

network into one that meets the requirements of positive pressure and water flow in all pipes. The results show the most vulnerable sectors, which are no longer functional following an earthquake. However, the nodal water flow demand remains unchanged before and after an earthquake. Therefore, the serviceability of the WSN may be overestimated.

2.5.2 Demand reduction

Another approach to solving the negative pressure problem in a damaged WSN is to reduce the demand at the nodes. The PDD model is a suitable approach for solving the problem. However, the calculation is based on nodal pressure rather than nodal demand; thus, a new hydraulic analysis algorithm is required because the commercial software does not provide the ability to perform this analysis. Therefore, the DR method was proposed to conduct hydraulic analysis using EPANET.

The iteration of the NPE method is based on the modification of WSN components, whereas the DR method is based on the modification of nodal demands. Two states are used in the analysis, i.e., nodal demands, which result in positive nodal pressure (D_{Posi}), and negative nodal pressure (D_{Nega}). Note that the state of the initial nodal demand is the D_{Nega}; otherwise, the iteration is not needed. At first, the demands for all nodes are set to 0.001 m^3/d, which is a relatively small value rather than zero, in order to avoid convergence problems. NPE analysis is conducted to eliminate the nodes and pipes that cannot be supplied. In this stage, the pressure on all nodes is positive, i.e., the initial D_{Posi}. Second, the water flows at residual nodes are determined iteratively. A hydraulic analysis is conducted with the new nodal demands that are half of the D_{Nega} and D_{Posi}. The value of D_{Nega} or D_{Posi} is updated after the analysis. If negative pressure exists, the D_{Nega} will be updated; otherwise, the D_{Posi} will be updated. The process continues until a tolerance of 0.005 m^3/d is satisfied, and no negative pressure nodes exist in the WSN.

2.6 Functionality assessment

The system functionality, F_s, is defined as a comprehensive indicator that reflects the states of all nodes that are supplied by the WSN; 0 represents the complete loss of functionality, and 1 denotes a fully operational WSN (Eq. (2)). The state of a node is determined by the satisfaction rates of water flow demand (D) and water pressure (P) of the node after and before an earthquake occurs. A coefficient α, ranging from 0 to 1, is introduced to indicate the relative importance of water flow and pressure (Eq. (3)). α =1 denotes that the function of the system is entirely determined by

nodal water demand, which is used in the GIRAFFE software. In contrast, α =0 indicates that nodal pressure dominates the functionality of the system. For example, the water demand and pressure of node *i* are 1,000 m^3/d and 35 m, respectively, prior to an earthquake. In a single Monte Carlo simulation, the water demand and pressure of the node are 500 m^3/d and 30 m, respectively, following the earthquake. Let α = 0.5, the functionality of the node 0.5×500/1,000+0.5×30/35=0.68. Different weight coefficients are assigned to the nodes and are standardized $\Sigma\varphi_i$ to unity. It should be noted that identical weight coefficients are generally used for different nodes. However, in some cases, especially in the WSN, the system′s functionality is highly dependent on some of the nodes due to their importance, either because the nodes have a higher water demand or they are used to supply water to important facilities such as hospitals. For simplicity, the weights of the nodes are calculated as the water flow of a node over the total supply of the WSN, as shown in Eq. (4):

$$F_s = \frac{\sum \varphi_i S_i}{\sum \varphi_i} \tag{2}$$

$$S_i = \alpha D_i + (1-\alpha) P_i \tag{3}$$

$$\varphi_i = \frac{D_i}{\sum D_i} \tag{4}$$

where φ_i is the weight coefficient of the *i*-th node, S_i is the operational state of the *i*-th node, D_i is the water flow demand ratio of the *i*-th node, and P_i is the water pressure ratio of the *i*-th node. α is the relative importance coefficient of demand and pressure.

Note that water demand can change dramatically after an earthquake happens. For example, the demand of nodes supplying hospitals and shelters may increase, whereas demand can be reduced due to policy issues, including do-not-drink orders, boil-water orders, or water conservation efforts (Klise *et al*., 2017). Nevertheless, we use the concept of functionality to quantify residual services provided by the damaged WSNs. System functionality prior to an earthquake is selected as the reference value; thus, demand variation is not considered.

3 Case study

3.1 Overview

A virtual city is used as a benchmark model to compare the resilience assessment results (Shang *et al*., 2020) since it is challenging to perform this analysis by using an actual city. This is due to factors of complexity, data accessibility, and limited knowledge and documentation. This virtual medium-sized city is located in the southeast coastal area of China, with an area of 345 km^2 and a population of 690,000. The design earthquake intensity level is VII. The PGA corresponds to a design-basis earthquake (DBE), and the maximum considered earthquakes (MCEs) are 0.10 g and 0.22 g, with exceedance probabilities of 10% and 2%, respectively in 50 years. The virtual city is located in an alluvial plain; thus, any differences in elevation can be ignored. Soil condition is categorized as type II in the Chinese code (GB 50011-2010, 2010). Soil liquefaction and other geological disasters are not considered.

The WSN, which includes 190 nodes and 323 pipes, is shown in Fig. 6. Water is supplied to the urban area by a water plant (WP) situated to the southwest, with a pumping station (PS) located to the southeast, with capacities of 200,000 m^3/d and 50,000 m^3/d, respectively. The water pressures of WP and PS are 38 m and 35 m, respectively. The pipes (total length of approximately 255 km) are made of CI (58%) and polyvinyl chloride (PVC, 42%), with diameters of 200–1000 mm, as shown in Table 1. The CI pipes were installed before 2010 and primarily serve more well-established parts of the city, including the important local business districts, which show a high population density. The PVC pipes were installed after 2010 in supply economic zones and new industrial areas.

3.2 System functionality before the earthquake

According to the Code of Urban Water Supply Engineering Planning (GB 50282-2016, 2017), the comprehensive water consumption of residential areas is 2,500 m^3/(10,000 people·d), and the water consumption of industrial land is 15 $m^3/(hm^2 \cdot d)$. The total water demand of the WSN is 209,000 m^3/d. The normal operational state of the WSN before an earthquake is shown in Fig. 7. The water demand of the nodes ranges from 105 to 2,780 m^3/d. The lowest water pressure is 30.5 m, satisfying the minimum service requirement of 28 m.

3.3 Repair rates of pipe damage

The damage to pipes, i.e., breaks and leaks, is simulated during hydraulic analysis rather than adding a specific leakage flow at the nodes. The buried pipelines cover a large area, with wide variability in site conditions. Therefore, the seismic vulnerability of the buried pipelines is evaluated by using the pipe RR. The water plant and the pumping station are assumed to be intact after the earthquake because the serviceability of the WSN will be reduced significantly if either of them is damaged during the earthquake. Such an assumption is used only to demonstrate the difference in the WSN's functionality by using the NPE method and the proposed DR method. Nevertheless, the seismic vulnerability of components other than pipelines will be

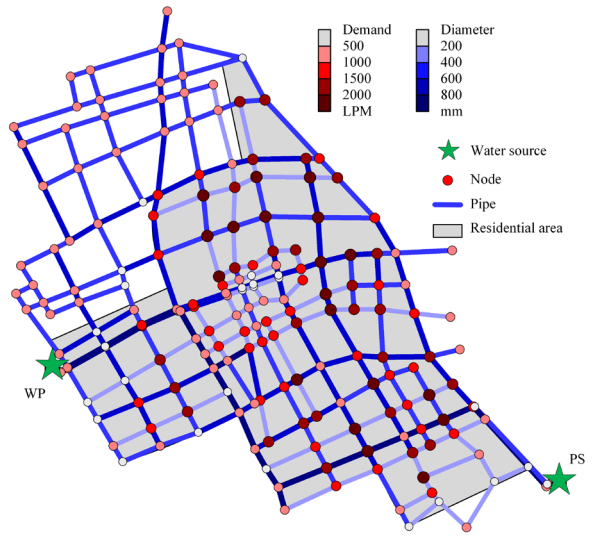

Fig. 6 Configuration of the water supply network

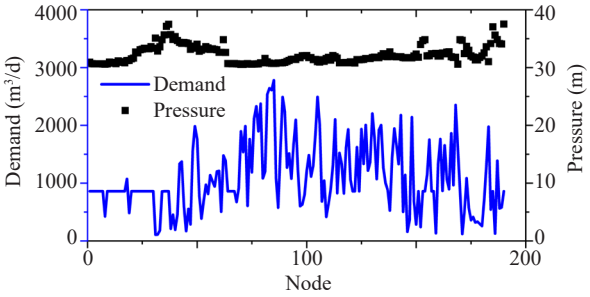

Fig. 7 Water demand and pressure of the WSN during normal operations

included in future studies. The damage states of these components will be determined based on PGA values and corresponding fragility curves (Yoo *et al.*, 2016b). For example, the fragility curves of water treatment plants, pumping plants, wells, and storage tanks are provided by FEMA (Federal Emergency Management Agency, 2003).

The JWWA model (Japan Water Works Association, 2009) that determines the RR based on the PGA is used for simplicity, as shown in Eqs. (5) and (6). Other empirical models such as the ALA model (American Lifeline Alliance, 2001) and the FEMA model (FEMA, 2003) can also be used based on the priorities of the study. Edinger (2015) and Mazumder *et al.* (2020) emphasize that the corrosion deterioration of pipe materials causes significant effects on the seismic performance of WSNs that were built earlier than 1960. However, the sample WSN were built after 1980. Therefore, the corrosion deterioration factor was not considered in this study. The virtual city is located on a flood plain, and the correction coefficient of topography and geology, C_g, is 1.0. The correction coefficients of the pipe material, C_p, are 1.0 for the CI and PVC pipes. No liquefaction is considered; thus, the C_y is 1.0. A correction coefficient of 0.8 is used for pipes with diameters of less than 500 mm; the correction coefficient of larger pipes is 0.5. The details of these two coefficients are shown in Table 4.

$$RR = C_p \times C_d \times C_g \times C_y \times R(\bullet) \tag{5}$$

$$R(\bullet) = 2.88 \times 10^{-6} \times (PGA - 100)^{1.97} \tag{6}$$

where C_p, C_d, C_g, and C_y are the correction coefficients of the pipe material, pipe diameter, topography and geology, and soil liquefaction, respectively.

An example of one of the damage scenarios of the WSN at 0.4 g is shown in Fig. 8, where 35 pipes of the WSN are damaged. Most of them sustain damage at only one location, except for three pipes, which sustain both break and leak damage and two pipes, which sustain two leaks. Note that the seismic hazard analysis is not included in the current study, but it is definitely important for the estimation of the serviceability of distributed civil infrastructure systems such as WSNs. When it is integrated into the analysis framework, the impact of spatial correlation and cross-correlation of the intensity measures will be discussed (Adachi and Ellingwood, 2009; De Risi *et al.*, 2018).

3.4 System functionality after the earthquake

The average functionality of the WSN based on the NPE method with 10,000 simulations after the earthquake (0.4 g) is shown in Fig. 9. Note that the weight coefficients of the nodes are not considered at this stage. The WSN's functionality is 0.97 if solely the nodal demands are considered, which are used in GIRAFFE. However, nodal pressure is small compared to that of the intact WSN. If only nodal pressure is considered, the system functionality is 0.24. The system functionality ranges from upper to lower limits when the relative

Table 4 Correction coefficients used in the JWWA model

Factor	Classification	Correction coefficient
C_p	Cast iron	1.0
	PVC	1.0
C_d	$200 \le D < 500$	0.8
	$D \ge 500$	0.2
C_g	Mountainous region	1.1
	Hilly area	1.5
	Former river	3.2
	Alluvial plain	1.0
	Stiff alluvial plain	0.4
C_y	No liquefaction	1.0
	Partial liquefaction	2.0
	Complete liquefaction	2.4

importance coefficient α is used. A sensitivity analysis was conducted to determine the number of required Monte Carlo simulations. The differences (Fig. 9) in the WSN's functionality for 200, 500, 1,000, 2,000, and 5000 simulations compared to 10000 simulations range from -4.31%–0.74% and -1.09%– -0.13% when α=0 and α=1 are used, respectively. Note that the errors of 2000 simulations are less than that of 5000 simulations when $\alpha < 0.5$. Therefore, 2,000 simulations were used in the following analysis, considering both accuracy and computational costs.

The average nodal functionality of the WSN based on the NPE method at 0.4 g is shown in Fig. 10. The water demand of more than 80% of the nodes can basically be met. However, the water pressure of approximately 75% of the nodes is less than 30%. If solely water demand is used as the evaluation index, the functionality of the WSN will be overestimated. However, it may be too conservative to only use nodal pressure. It would be more reasonable and accurate to use a combination of both factors. The determination of the combination coefficient (α), however, needs further study from engineering practice, which may change according to the demand from users, engineers or regulators. The analysis methods and results should be calibrated by actual data that is observed during earthquakes. Some nodes (such as node 37) are close to or even directly connected to the BS; thus, the functionality of these nodes is significantly higher than that of others.

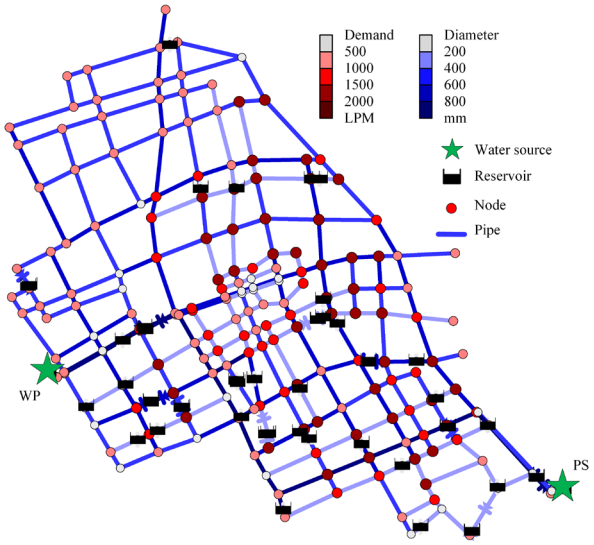

Fig. 8 Damage distribution of the WSN at 0.4 g

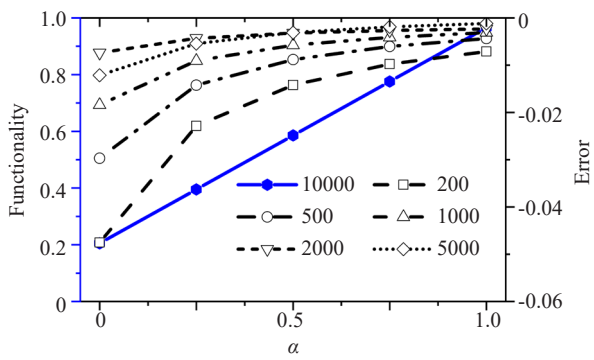

Fig. 9 Functionality of the WSN and sensitivity analysis at 0.4 g

4 Discussion

4.1 Comparison of the NPE and DR method

The average nodal functionality of the WSN based on the DR method at 0.4 g is shown in Fig. 11. The water demand of 92% of the nodes is reduced to 0.90, which is considerably different from the results of the NPE method. However, the average nodal pressures are almost the same as those using the NPE method, which indicates the capacity of the damaged WSN to supply water.

The standard deviations of nodal functionality based on the NPE and DR methods are shown in Figs. 12

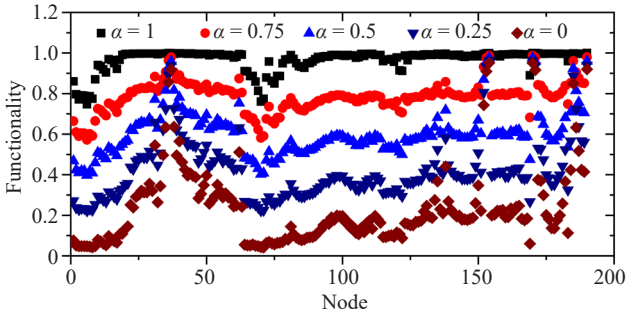

Fig. 10 Nodal functionality at 0.4 g using the NPE method

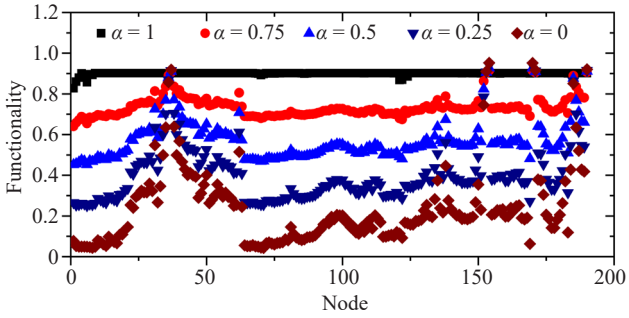

Fig. 11 Nodal functionality at 0.4 g using the DR method

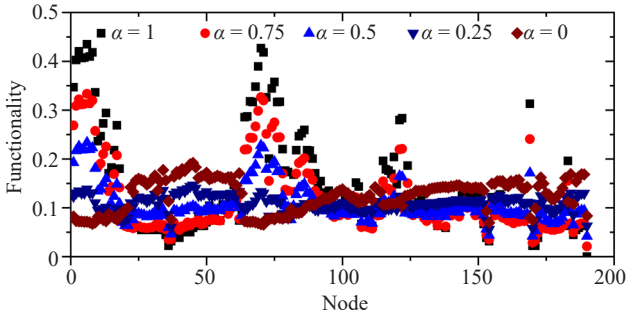

Fig. 12 Standard deviation of nodal functionality at 0.4 g using the NPE method

and 13, respectively. The standard deviations of nodal functionality based on the NPE method range from 0.02 to 0.44, whereas those of the DR method range from 0.19 to 0.34. In the DR method, the standard deviations of more than 80% of the nodes are 0.19, which indicates that fewer Monte Carlo simulations are required for the DR method than for the NPE method. The modified configurations of the WSNs after one simulation, using the two methods, are shown in Figs. 14 and 15, respectively. Note that the NPE process has eliminated most of the pipelines; by contrast, the WSN remains mostly intact when the DR method is used. Because the damage scenarios of the WSN are randomly generated, the modified system may be different in different simulations using the NPE method; thus, a large standard deviation of the nodal functionality is obtained.

According to Eq. (6), no damage will occur to the pipelines if the PGA is less than 0.1 g. Therefore, the WSN will be fully operational at the intensity of the DBE. The average functionalities of the WSN at 0.22 g, 0.3 g, and 0.4 g are shown in Fig. 16. At small PGAs of 0.22 g and 0.3 g, the system functionalities of the WSN obtained by the two methods are similar because there are few damaged pipelines, and there is probably no negative pressure in the system. At 0.4 g, as discussed before, the pressure values calculated by the two methods are almost the same, whereas the node demand is lower for the DR method. In this stage, the NPE method may overestimate the capacity of the WSN to supply water because it uses only nodal demand as an indicator.

4.2 Weight coefficient

Equal weights of the nodes are used in the above analysis. However, some nodes are more important than others, either because they deliver more water or because they deliver water to important facilities, such as hospitals. Therefore, the influences of the weight coefficients are determined. For simplicity, the weights are determined as the water flow of a node divided by the water flow of all nodes. The functionalities of the WSN with and without weight coefficients using the DR method are shown in Fig. 17. The functionality of the WSN is slightly lower when the weights are used because the nodes that supply a higher water flow contribute more to the system. The differences between the functionality with and without weights increases as the PGA increases in small values, i.e., 0.68%, 1.75%, and 2.87% at 0.22 g, 0.3 g, and 0.4 g, respectively, for $\alpha = 0.5$.

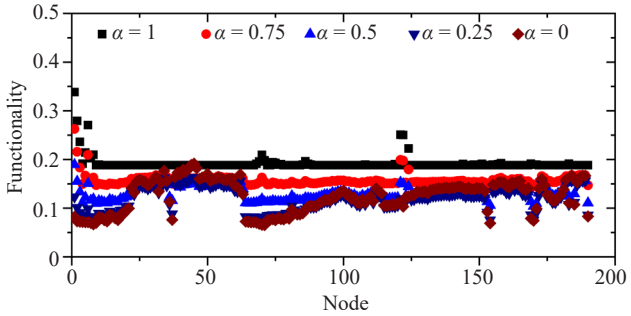

Fig. 13 Standard deviation of nodal functionality at 0.4 g using the DR method

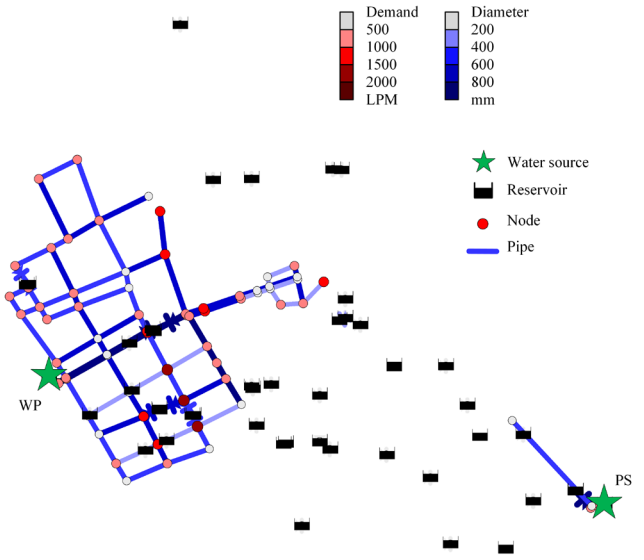

Fig. 14 Modified WSN configuration using the NPE method

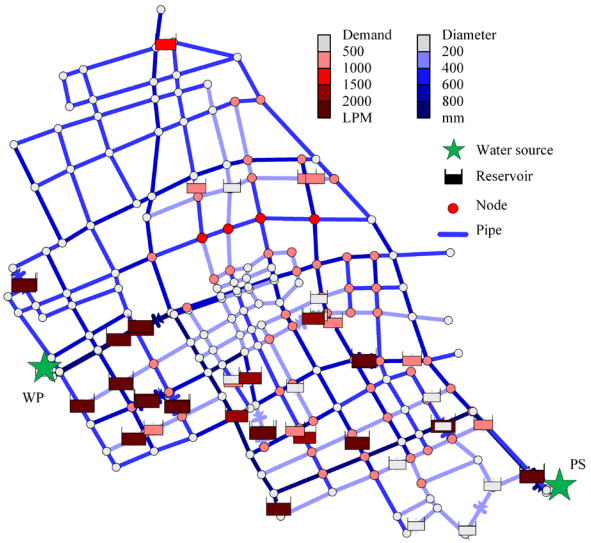

Fig. 15 Modified WSN configuration using the DR method

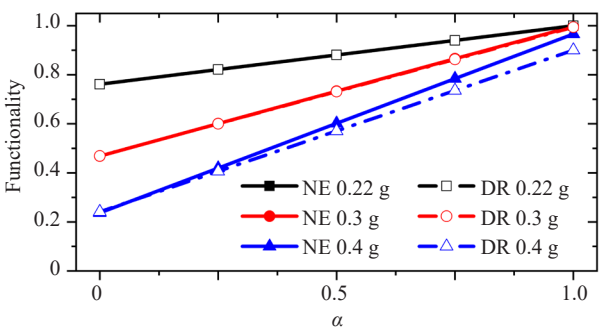

Fig. 16 System functionality at 0.22 g, 0.3 g, and 0.4 g using the NPE and DR methods

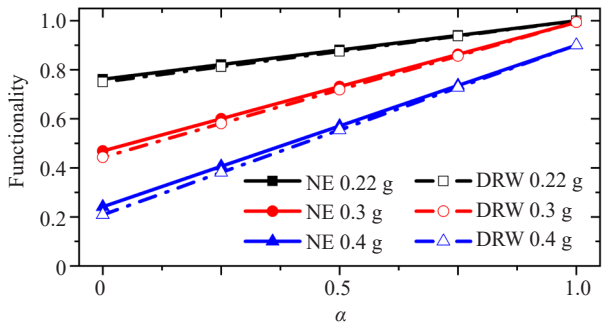

Fig. 17 System functionality with and without nodal weight coefficients at 0.22 g, 0.3 g, and 0.4 g using the DR method

5 Conclusions

A new probability-based framework was proposed to assess the functionality of WSNs. A new functionality quantification index that considers both nodal water flow and nodal pressure was used, and an importance coefficient that reflects the relative contributions to the functionality was incorporated. The DR method, which reduces nodal demand to avoid negative pressure problems in a severely damaged WSN, was proposed.

A case study was conducted on a WSN in a benchmark city for seismic resilience assessment. The influences of the nodal and system functionality were evaluated, and the use of two methods to deal with negative pressure in a damaged WSN was investigated.

The main conclusions are as follows:

(1) The system functionality should consider both water flow and water pressure of the nodes, which respectively determine the upper and lower limits of the WSN′s capacity to supply water. The functionality of the WSN was 0.24–0.97, with different relative importance coefficients at 0.4 g. The NPE method, which uses nodal demands as the serviceability indicator, overestimated the WSN′s capacity to supply water.

(2) The NPE and DR method exhibited no differences in the functionality at small PGA values of less than 0.3 g because the WSN was only slightly damaged. However, the pipe network was significantly damaged in a strong earthquake, i.e., 0.4 g. The NPE method eliminated most of the pipe segments, which was an unrealistic solution. As a result, the standard deviation of system functionality was higher for the NPE method than for the DR method. Fewer simulations were required for the DR method than was the case with the NPE method.

(3) The importance of the nodes that supply large amounts of water was determined using nodal weight coefficients. Although the influences of the weights increased as the PGA increased, the differences between the functionality with and without weights were small, i.e., 0.68%, 1.75%, and 2.87% at 0.22 g, 0.3 g, and 0.4 g, respectively, for $\alpha = 0.5$.

This study represents a preliminary analysis of the seismic resilience of WSNs, which quantifies the functionality of the WSN. The following topics should be investigated in future studies: (1) A real WSN with an actual seismic scenario is deemed necessary to demonstrate the efficiency and limitations of the methodology. (2) A seismic hazard analysis that considers the spatial distribution of the ground motion parameters should be included. Additional intensity measures, such as the PGV and PGD instead of the PGA should be used. (3) A quantification of seismic resilience that focuses on the recovery strategy to rapidly restore the functionality of the WSN should be performed. It is necessary to determine the time and cost to repair different types of pipe damage and consider the human, financial, and material resources. (4) Optimization of the configuration of the WSN should be conducted to ensure the reliability of the WSN and its resistance to earthquake damage.

Acknowledgement

The study was sponsored by the Scientific Research Fund of the Institute of Engineering Mechanics, China Earthquake Administration (2019EEEVL0505); the National Natural Science Foundation of China (51908519); and the Scientific Research Fund of the Institute of Engineering Mechanics, China Earthquake Administration (2019B02).

References

Adachi T and Ellingwood BR (2009), "Serviceability Assessment of a Municipal Water System Under Spatially Correlated Seismic Intensities," *Computer-Aided Civil and Infrastructure Engineering*, **24**(4): 237–248.

American Lifelines Alliance (2001), "Seismic Fragility Formulations for Water Systems: Part 1 - Guideline," *ACSE*.

Chen LL and Li J (2003), "Leakage Analysis of Water Supplying Networks," *Earthquake Engineering and Engineering Vibrations*, **23**(1): 115–121. (in Chinese)

Chen LL and Li J (2004), "Aseismatic Serviceability Analysis of Water Supply Network," *Engineering Mechanics*, **21**(4): 45–50. (in Chinese)

De Risi R, De Luca F, Kwon OS and Sextos A (2018), "Scenario-Based Seismic Risk Assessment for Buried Transmission Gas Pipelines at Regional Scale," *Journal of Pipeline System and Engineering Practice*, **9**(4): 04018018.

EERI (1995), "Northridge Earthquake of January 17. 1994 Preliminary Reconnaissance Report," *Earthquake Spectra*, Supplement C to V0.11.

Eidinger JM (2015), "Fragility Models that Reflect Pipe Damage in the 2014 Napa M 6.0 Earthquake," Accessed December 12, 2018. *https://www.geengineeringsystems.com/ewExternalFiles/Napa%202014%20Pipe%20Fragility.pdf*.

FEMA (2003), "HAZUS-MH Multi-Hazard Loss Estimation Methodology, Earthquake Model - Technical Manual," *Washington D.C., Federal Emergency Management Agency*, Department of Homeland Security.

Gao HY (2000), *GIS-Based Seismic Performance Analysis of Water Delivery Systems*, Harbin: Institute of Engineering Mechanics, China Earthquake Administration. (in Chinese)

GB 50011-2010 (2010), *Code for Seismic Design of Buildings*, Beijing: China Architecture and Building Press. (in Chinese)

GB 50282-2016 (2017), *Code of Urban Water Supply Engineering Planning*, Beijing: China Planning Press. (in Chinese)

GIRAFFE User's Manual (Version 4.2) (2008), *School of Civil & Environmental Engineering*, Cornell University.

Guo ED, Wang XJ, Zhang LN, *et al*. (2008), *Technical Report of the Scientific Investigation Team on Water Supply System in the Wenchuan Earthquake*, Harbin: Institute of Engineering Mechanics, China Earthquake Administration. (in Chinese)

Hou BW (2014), "Seismic Performance Assessment and Performance-Based Design of Water Distribution System," *PhD Dissertation*, Beijing: Beijing University of Technology. (in Chinese)

Hwang HHM, Lin H and Shinozuka M (1998), "Seismic Performance Assessment of Water Delivery Systems," *Journal of Infrastructure Systems*, **4**(3): 118–125.

Japan Water Works Association (JWWA) (2009), *Guidelines and Interpretation of the Anti-Seismic Construction Method for Waterworks* (*2009 edition*). (in Japanese)

Javanbarg MB (2008), "Integrated GIS-Based Seismic Performance Assessment of Water Supply Systems," *PhD Dissertation*, Kobe University, Kobe, Japan.

Javanbarg MB and Takada S (2009), "Seismic Reliability Assessment of Water Supply Systems," *Proceedings of 10th International Conference on Structural Safety and Reliability*, Osaka, Japan: IEEE, 3455–3462.

Klise KA, Bynum M, Moriarty D and Murray R (2017), "A Software Framework for Assessing the Resilience of Drinking Water Systems to Disasters with an Example Earthquake Case Study," *Environmental Modelling & Software*, **95**: 420–431.

Laucelli D and Giustolisi O (2015), "Vulnerability Assessment of Water Distribution Networks Under Seismic Actions," *Journal of Water Resources Planning and Management*, **141**(6): 04014082.

Laucelli D, Berardi L and Giustolisi O (2012), "Assessing Climate Change and Asset Deterioration Impacts on Water Distribution Networks: Demand-Driven or Pressure-Driven Network Modeling?" *Environment Model Software*, **37**: 206e216.

Li HN, Xiao SY and Huo LS (2008), "Damage Investigation and Analysis of Engineering Structure in the Wenchuan Earthquake," *Journal of Building Structures*, **29**(4): 10–19. (in Chinese)

Li J (2005), *Earthquake Resistance of Lifeline System: Theory and Application*, Beijing: Science Press. (in Chinese)

Li J, Wei SL and Liu W (2006), "Seismic Reliability Analysis of Urban Water Distribution Network," *Earthquake Engineering and Engineering Vibration*, **5**(1): 71–77.

Liu CG and He SH (2010), "Hydraulic Analysis of Urban Water Supply Network After Strong Earthquakes," *World Earthquake Engineering*, **02**: 27–31. (in Chinese)

Liu HX (1986), *Damage in the 1976 Tangshan Earthquake*, Beijing: Earthquake press. (in Chinese)

Liu W, Zhao YG and Li J (2015), "Seismic Functional Reliability Analysis of Water Distribution Networks," *Structure and Infrastructure Engineering*, **11**(3): 363–375.

Mazumder RK, Fan X, Salman AM, Li Y and Yu X (2020), "Framework for Seismic Damage and Renewal Cost Analysis of Buried Water Pipelines," *Journal of Pipeline Systems Engineering and Practice*, **11**(4): 04020038.

Markov I, Grigoriu MD and O′Rourke TD (1994), "An Evaluation of Seismic Service Ability of Water Supply Network with Application to San Francisco Auxiliary Water Supply System," *NCEER-94-0001*, National Center for Earthquake Engineering Research, State University of New York at Buffalo, Buffalo, NY, USA.

Nuti C, Rasulo A and Vanzi I (2010), "Seismic Safety of Network Structures and Infrastructures," *Structure and Infrastructure Engineering*, **6**(1-2): 95–110.

Pathirana A (2011), "EPANET2 Desktop Application for Pressure Driven Demand Modeling," *Proceedings of the 12th Annual Conference of Water Distribution System Analysis 2010*, Tucson, AZ, USA.

Rossman LA (2000), *EPANET 2 User's Manual*, National Risk Management Research Laboratory, Office of Research and Development, U.S. Environmental Protection Agency, Cincinnati, OH, USA.

Romero N, O′Rourke T, Nozick LK and Davis CA (2010), "Seismic Hazards and Water Supply Performance," *Journal of Earthquake Engineering*, **14**(7): 1022–1043.

Scawthorn C (2011), "Water Supply in Regard to Fire Following Earthquakes," *Technical Report 2011-08*, Pacific Earthquake Engineering Research Center, Berkeley, California.

Shang QX, Guo XD, Li QW, *et al*. (2020), "A Benchmark City for Seismic Resilience Assessment," *Earthquake Engineering and Engineering Vibrations*, **19**(4): 811–826.

Sheldon MR (2000), "Introduction to Probability and Statistics for Engineers and Scientists," *20nd Edition*, Harcourt and Technology Company, San Diego, CA, USA.

Shi P and O'Rourke TD (2008), "Seismic Response Modelling of Water Supply Systems," *Technical Report MCEER-08-0016*, Multidisciplinary Center for Earthquake Engineering Research, Buffalo, NY, USA.

Shinozuka M (1995), "The Hanshin-Awaji Earthquake of January 17, 1995: Performance of Lifelines," *Technical Report MCEER-95-0015*, US National Center for Earthquake Engineering Research, Buffalo, NY, USA.

Shirzad A, Tabesh M, Farmani R and Mohammadi M (2013), "Pressure-Discharge Relations with Application to Head-Driven Simulation of Water Distribution Networks," *Journal of Water Resources and Planning Management*, **139**(6): 660–670.

Trifunovic N (2012), "Pattern Recognition for Reliability Assessment of Water Distribution Networks," *PhD Dissertation*, Delft University of Technology, Delft, Netherlands.

Wang Y and Au SK (2009), "Spatial Distribution of Water Supply Reliability and Critical Links of Water Supply to Crucial Water Consumers Under an Earthquake," *Reliability Engineering and System Safety*, **94**(2): 534–541.

Wham BP and TD O'Rourke (2016), "Jointed Pipeline Response to Large Ground Deformation," *Journal of Pipeline System and Engineering Practice*, **7**(1): 04015009.

Xu C and Goulter IC (1998), "Probabilistic Model for Water Distribution Reliability," *Water Resources Planning and Management*, **124**(4): 218–228.

Yoo DG, Jung D, Kang D and Kim JH (2016a), "Seismic-Reliability-Based Optimal Layout of a Water Distribution Network," *Water*, **8**(2): 50.

Yoo DG, Jung D, Kang D, Kim JH and Lansey K (2016b), "Seismic Hazard Assessment Model for Urban Water Supply Networks," *Journal of Water Resources Planning and Management*, **142**(2): 04015055.

Zhang XK (2004), *Seismic Damage Analysis of Urban Water Supply System*, Beijing: Beijing University of Technology. (in Chinese)

Zhou Yi, Chen Yongxiang and Li Xi (2011), "Pressure Driven Water Demand Calculation in Water Supply Network," *Engineering Journal of Wuhan University*, **01**: 82–85. (in Chinese)